

Progressive observation of Covid-19 vaccination effects on skin-cellular structures by use of Intelligent Laser Speckle Classification (ILSC) method

Ahmet Orun (Corresponding Author)

De Montfort University, Faculty of Computing, Engineering and Media, Leicester UK, LE1 9BH

Email: aorun@dmu.ac.uk. Phone: +44(0)116 3664408

Fatih Kurugollu

University of Sharjah, Department of Computer Science

Sharjah, UAE, UK. Email: fkurugollu@sharjah.ac.ae

Abstract

The recent pandemic showed that the current global research strategies on vaccine development necessitates more optimized supplementary techniques to observe instant progressive vaccines' subtle effects on human metabolism, for better evolutionary assessments. To fill this gap, we have followed a multi-disciplinary approach exploiting AI, laser-optics, and a specific imaging method. The proposed technique is able to make progressive observations on Covid-19 Astra Zeneca vaccination effects on skin cellular network by use of the well-established technique - *Intelligent Laser Speckle Classification (ILSC)*, as Covid-19 is a skin-affecting systemic disease. The method also managed to distinguish between three different subject groups via their laser speckle skin image samplings, grouped as: early-vaccinated, late-vaccinated and non-vaccinated participants. The results have proven that the *ILSC* technique, in association with the parametrically optimised Bayesian network, is capable of classifying hidden skin changes of vaccinated and non-vaccinated individuals up to 90% accuracy and is also capable of detecting instant (real-time) progressive developments pertaining to skin cellular properties.

Keywords: Skin cells, Covid-19 Vaccine, laser speckle imaging, Bayesian Nets.

1 Introduction

Covid-19 infection or its vaccine's effect on the skin structure and components had already been studied earlier and proven by several authors (Sun et al., 2021; Magro et al., 2021; Bogdanov et al., 2021) as Covid-19 is a systemic disease whose signs are also reflected by the skin. However the recent Covid-19 pandemic event has proven that, a more effective and speedy diagnosis or detection of such systemic diseases is inevitable, which could only be done by a non-destructive instant skin analysis using optical imaging methods (Orun et al., 2014; Orun, 2014) rather than microscopic inspection with biopsies that cannot be applied non-destructively in real-time. In the previous studies, Magro et al. (2021) made a comprehensive analysis of the Covid-19 effects on skin by using light microscopy for skin biopsies but their method targeted neither an instant disease diagnosis nor an observation of its prognosis. In another work, Bogdanov et al. (2021) focused on the adverse effects of the Covid-19 vaccine on the skin. Their research was based on basic visual inspection or biopsy techniques. Almost all other global studies on Covid-19 vaccines effect (Lospinoso et al., 2021) mainly rely on visual inspections and biopsies which require highly equipped clinical environments and high-cost medical instrumentation. Within this research, we propose an alternative non-destructive optical "instant observation" technique of Covid-19 vaccine effects by use of Intelligent Laser Speckle Classification (*ILSC*) which could be potentially used for the diagnosis and prognosis of Covid-19 disease in a particular period of time-sequence.

The laser speckle technique has several advantages over the other traditional optical methods (Millet et al., 2011) for the skin analysis such as, due to its specifically selected wavelength ($\lambda=0.65\mu\text{m}$) smaller than skin cells (30 μm), the laser light can interact with the skin cellular network to detect its micro changes as a textural phenomenon rather than focusing on a single cell alone (Orun et al., 2014). This ability provides a power of ultra-high sensitivity and high spatial resolution to observe a network of very small units like skin cells or even their sub-cellular features (e.g. cell's nuclei, cell membranes, etc.). The advantage of lasers over an ordinary broad spectrum (non-coherent) light sources are well known characteristics (Ginouves, 2003) this is due to the micro level interaction of lasers with skin features and its deep penetration into biological tissues. The proposed system also consists of basic level instrumentation (e.g. camera at specific spectral sensitivity, specific laser source, auxiliary optical components) and is highly competitive against high-cost and non-real-time techniques like electron microscopy, optical tomography, ultrasound, Raman microscopy, etc. By the integration of Bayesian AI

capability with laser speckle imaging technique as is then called “Intelligent laser speckle classification” (*ILSC*), the method becomes more efficient for textural features classification. *ILSC* is an integrated technique (Orun et al., 2014a, 2014b, 2016, 2017) which comprises different disciplinary methods providing high sensitivity and discrimination power to detect subtle differences even at the sub-cellular level. The method detects laser speckles’ textural differences, not for only a single cell unit but rather on the whole cellular network to detect any common property or structural changes in all cells simultaneously since all cells are naturally identical to each other or react to external effects in same way. To increase the physical detection sensitivity, the most suitable laser wavelength has to be selected. In our case red laser light ($\lambda=0.65 \mu\text{m}$) is used as an optimum one for human skin and blood cells analysis (Butkus, 2003). The most important advantage of the method is its non-invasive real-time continuous observation by a *CCD* camera-laser source based simple optical configuration. Figure 1 depicts the image acquisition setup configuration as is used to acquire Laser speckle images of the cellular network with pixel window samplings. The laser wavelength $\lambda=650 \text{ nm}$ is shorter than individual cell size ($\sim 30\mu\text{m}$) or sub-cellular components size (e.g. nucleus) so that the laser light penetrates inside the skin surface ($\sim 0.56\text{mm}$) then interacts and causes backscattering by conveying the characteristic information of cellular components back to the image domain. The surface normal makes 23° angles with a laser beam and camera viewing axis. We have to note that the angular degrees are not specifically selected but they have to be kept constant at all times as laser speckle’s physical phenomenon is extremely sensitive against angular changes (Dainty, 1984).

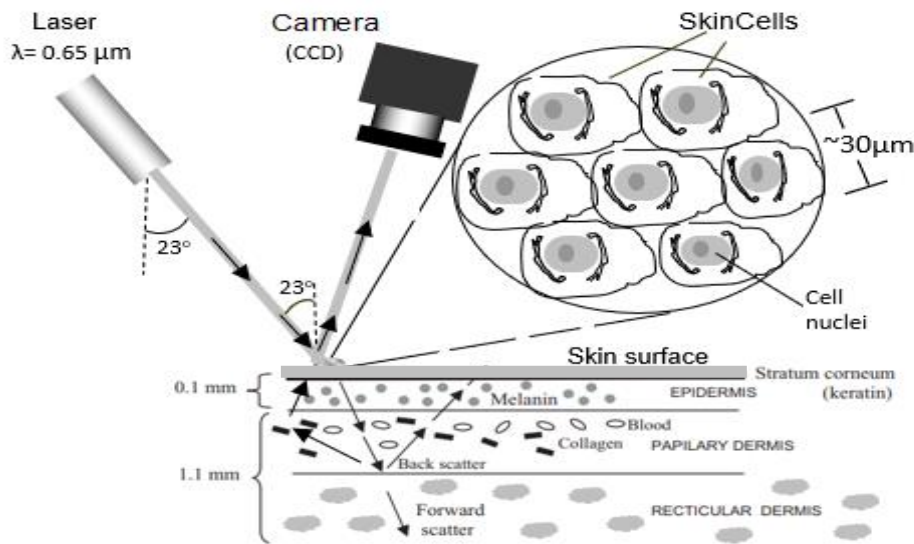


Figure 1. Image acquisition setup configuration with the basic system components (laser wavelength $0.65 \mu\text{m}$ which corresponds to 650 nm in the text). The optical angular degrees are arbitrarily selected but to be kept constant in the system.

Like some of the most important global diseases (e.g. diabetes, heart disease, kidney disorder, etc.) The Covid-19 disease is also a systemic disease whose effect is reflected by skin surface (Mohamed et al., 2021). That is fortunately a supportive argument for this study where the Covid-19 vaccination progressive effects as normally invisible to the human eye can be observable as it causes cellular structural changes. The other effects like an increase of antibodies in the blood, changes in blood capillary loops, etc. may also be observable by *ILSC* technique. According to the AstraZenecaTM report (AstraZeneca, 2021), a single dose of vaccination leads to a four-fold increase in antibodies in 95% of participants in one month after injection. Hence the tests used in this study covers one month period after the first injection. The main contributions of this research to the earlier studies would be as follows:

- Within this research, we have proven that the Covid-19 vaccine effect and possibly Covid-19 infection can be observable at high frequency of data collection, with high reliability. “Multi-Classifer System” (MCS) is also applicable by the addition of more laser sources with different wavelengths (e.g. red, IR, etc.) (Orun and Smith, 2017; Wozniak et al., 2014; Ho et al., 1994).
- Speedy image acquisition and processing provide a real-time skin analysis which enabling a continuous skin observation by successive data collection.
- Texture based laser speckle image classification provides very high spatial resolution with “scalability” for the analysis of sub-cellular features (depending on specifically selected laser wavelength)
- The Laser speckle effect is a physical phenomenon which is very sensitive against the subtle changes in any textural features like skin cellular network, whose potential is exploited within this work.

- Even though the classification capability of the system is proven by Bayesian networks here, such AI components can easily be replaced by other methods (e.g. deep learning – Convolutional NN, etc.).
- Skin penetration of the laser light would also be depending on its selected wavelength. This provides a filtering capability of unwanted skin layers' obstruction for the ideal image data acquisition (Bashkatov, 2005).

1.1 Covid-19 and its vaccine effects on skin

After the coronavirus global spreading effected nearly 145 million people at the time of April 2021, the first doses of human Covid-19 vaccine were started to be tested in March 2020 (Tregoning et al., 2020). Meanwhile the United Kingdom was the first country to approve and test Pfizer-BioNTech vaccine (Ledford et al.,2020) and it was followed by vaccination of Oxford-AstraZeneca in January 2021 after approval of World Health Organisation (World Health Organisation, 2020). Meanwhile the vaccines' side effects onto the skin have been recently studied with the Worldwide coverage (Sun et al.,2021). Some of the conclusions were made that, the most common skin reactions cited by the clinical trial data were as follows; delayed large local reactions (4 days or more after vaccination), pityriasis-rosea-like eruptions, reactivation of herpes simplex, varicella zoster (McMahon et al.,2021). According to the trial reports, Oxford-AstraZeneca (AZD1222) vaccine caused very rare skin side effects of severe cellulitis, psoriasis, rosacea, vitiligo and Raynaud phenomenon (Voysey et al.,2021). The studies have also proven that the cutaneous (skin) reactions like eruptions caused by Covid-19 vaccine have similarity with the mild and moderate Covid-19 skin symptoms (Magro et al.,2021). It was reported that up to 20% of patients with Covid infection also suffered from skin eruptions (Zhao et al.,2020)

2 Materials and methods

The methodology covers three main tasks within this research such as; 1) Specification of laser reflection parameters to optimise light-skin interaction which involves fundamental light physics. According to fundamental principles, the frequency of light ($f = C / \lambda$ where C: light speed, λ : light wavelength) has to be different than the Atomic (electrons) frequency of skin properties for its reflection from the skin, otherwise light is absorbed. Meanwhile laser speckle modelling is a more complex one than normal light reflection as described by Equations 1-3 in Chapter 2.2. 2) Laser speckle image (LSI) analysis includes optimized image sampling at the best energy band (broad enough with max number of laser speckle primitives) as shown in Figure 3. And also selection of most suitable texture measures for LSI texture analysis for the image quantisation process. 3) The final task refers to Bayesian (AI) classification technique which is a qualitative process to make a comparison between the subject groups.

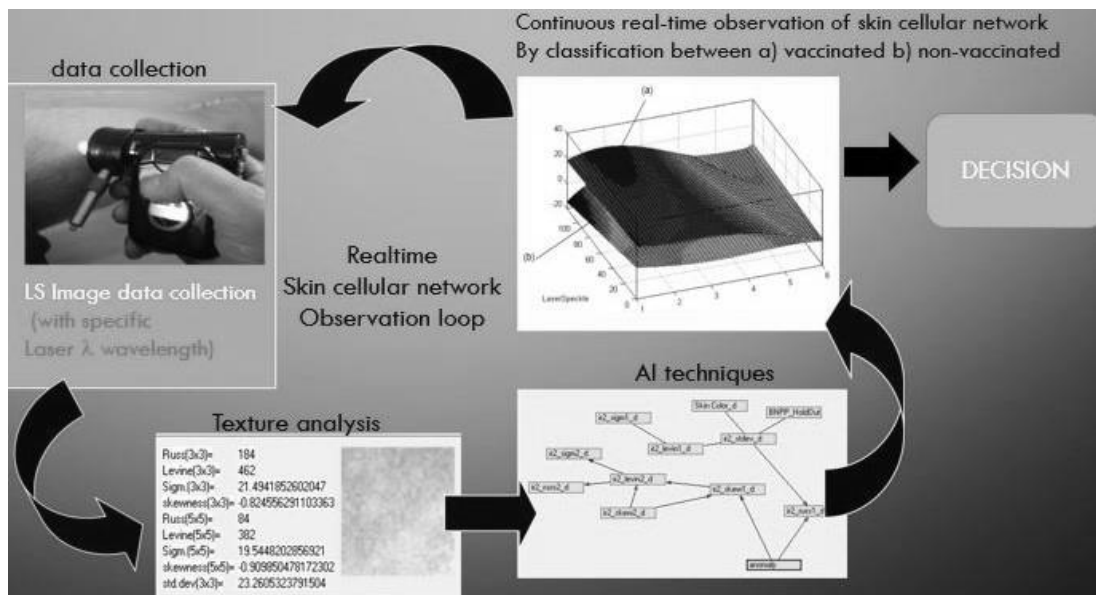


Figure 2. Real-time Skin cellular network analysis loop by which the system provides instant decision on skin cellular network abnormality caused by Covid-19 infection. The operation enables real-time parametric skin observation

2.1 Laser speckle imaging camera system

For the laser speckle image data acquisition, a high resolution (3840×2880 pixels) commercial *CCD sensor* image camera is used where each CCD pixel corresponds to $2.8 \mu\text{m}^2$ area on the image domain. The camera is utilized after a moderate modification by attaching a low level laser source (1mW power) with approximately 23° of angle to the skin surface normal which is fixed arbitrarily at the system design stage where such incident/reflection angle degree level has no any quality effect on the measurements unless they are extremely wide or narrow but those angles have to be kept constant permanently (Fig. 1). The laser source is a collimated red laser diode at 650 nm wavelength (Bashkatov et al.,2005) whose power is much less than maximum permissible exposure which is 2000 Wm^{-2} for human skin (at 400–700 nm wavelength range) for a long term exposure such as between 5–10 hours. The laser source is used in our tests only for short-term illuminations (approx. 3–5 seconds) over approximately 10 mm diameter area on the upper-hand skin of each participant to generate a speckle effect on the skin surface and sub-skin layers. The skin imaging location of upper-hand is selected since the same body region has been used in our earlier skin related (non-Covid) studies yielding the accurate results (Orun et al., 2014; 2016)

2.2 Laser speckle phenomenon

As far as the basic principle of “laser light-skin surface interaction” is concerned, when a skin surface is illuminated by a coherent light like laser then the light itself penetrates inside the skin and scatters from the skin layers exhibiting a particular intensity distribution as it looks covering the skin surface with a granular structure. The very fundamental formula of laser speckle image includes its pixel intensity statistics (1), where the standard deviation of spatial intensity variations σ_s is equal to the mean intensity $\langle I \rangle$ for a fully developed (ideal) speckle pattern. This would be stated by the basic formula (1);

$$K = \sigma_s / \langle I \rangle \quad (1)$$

where K is the speckle contrast and its value takes place between 0 and 1. If the speckle pattern is ideal then $K=1$. But if the speckle pattern becomes not ideal such as blurred by a diffuser or surface motion, the value of K will be shifted towards zero. The laser speckle effect image formation and its statistical analysis at the skin observation domain by use of a digital camera (e.g. CCD ideally or CMOS at lower cost but less accurate) is a multi-parametric task. The laser speckle image’s statistical property heavily depends on its system geometry like laser illumination angle or camera orientation. In the image formation domain a basic light amplitude at point A (e.g. at a single pixel of CCD camera matrix) may be formulized as in Formula 2 and 3 (Orun and Alkis, 2003);

$$I_j(A) = |I_j| e^{i\varphi_j} \quad (2)$$

The complex amplitude I_{com} in the image domain at point A would be written as ;

$$I_{\text{com}}(A) = \frac{1}{\sqrt{N}} \sum_{j=1}^N |I_j| e^{i\varphi_j} \quad (3)$$

where;

- I_j : Basic light amplitude of a surface element j
- A : Point on image domain (single pixel of CCD matrix)
- φ_j : Random phases of light at j^{th} surface element.
- i : Imaginary part
- N : Total surface elements

2.3 Texture analysis of LSI

Image texture analysis (Phillips, 1995) utilizing specific texture measures is the essential and initial part of the Intelligent laser speckle classification (ILSC) technique that was tested and used successfully in last nearly two decades with high accuracy (Orun and Smith, 2017; Orun and Alkis, 2003). The formulations are described by the Equations 4-8. The nine types of texture measures used based on the Formulas 4-8, five texture measures with 3×3 pixel image scanning kernel, and four texture measures with 5×5 pixel kernel in association with all those formulas. The texture measures are applied on 30×30 pixel image segment of each laser speckle image where the

laser speckle effect appears to be at maximum level (Figure 3). Sampling process of the laser speckle images has a great importance where the uniform textural characteristics of image segment should be justified. To optimize this task, each 30x30 pixel sampling area should have sufficient number of texture primitives and also textural uniformity all over the area (Orun et al., 2014).

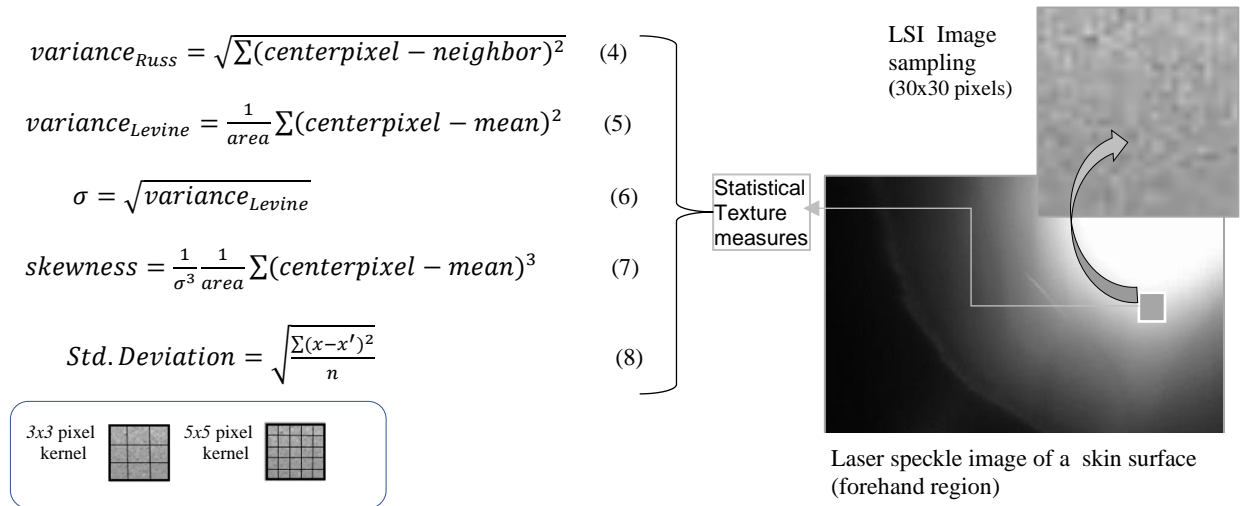


Figure 3. Pixel based arithmetical operators (on the left) for the image texture measures are applied on each laser speckle skin image sampling. Each 30x30 pixel image sampling is selected on the global laser illuminated image area where the physical laser speckle effects particularly exist as shown in the square region of interest (on the right)

2.4 Bayesian Networks as applicable AI method

Bayesian Network (BN) is well established Artificial Intelligent method whose details and statistical description are already given in several publications (Drugan and Wiering, 2010; Jensen; 1998; Orun and Seker, 2012) The most remarkable characteristics and advantages of Bayesian Networks are that it can demonstrate knowledge representation and reasoning even under high uncertainties, and it also provides a graphical representation of links between the related attributes. In BN, each node refers to data attribute or called variable as those variables are connected to each other via links (arcs) representing dependency relationships between them. BN's structure can be explained as follows: if $A=\{X_1, \dots, X_n\}$ is a random variable denoting the patterns covering the $n = N \times M$ dimensional vector space, then joint probability distribution $P=(X_1, \dots, X_n)$ will be a product of all conditional probabilities whose Equation 9 would be ;

$$P(X) = \prod_i P(X_i | pa(X_i)) \quad (9)$$

Where; $pa(X_i)$ is parent set of X_i . As a brief, Bayesian algorithm examines the information of two related variables from a data set and decides if two variables are dependent. It also investigates how close the relationship is between those variables. This information is called conditional mutual information of two variables X_i, X_j which may be denoted as:

$$I(X_i, X_j | C) = \sum_{x_i, x_j, c} P(x_i, x_j, c) \log \frac{P(x_i, x_j | c)}{P(x_i | c)P(x_j | c)} \quad (10)$$

In Equation 10, C is a set of nodes and c is a vector (one instantiation of variables in C). If $I(X_i, X_j | C)$ is smaller than a certain threshold t , then we can say X_i and X_j are conditionally independent. Bayesian Networks are also called belief networks, casual probabilistic networks or directed Markov fields. The utilities called PowerPredictor™ and PowerConstructor™ are used within the experiments in this study as they refer to Bayesian Classifier (Figures 4, 5 and 6) and Bayesian Inference system (Figure 7) respectively.

2.5 Laser-Optical Skin analysis

Optical imaging methods in association with a coherent light like lasers are very efficient tools for skin and sub-skin analysis and progressive observation as utilized by earlier applications (Orun et al.2014). As far as the coherent light and its skin interaction is concerned, the laser light has potential to penetrate deep into skin layers keeping its constant wavelength and causes specular reflection, diffraction and diffusely reflection from the skin layers then come back to skin surface. The generic physical phenomenon of light-surface interaction has been studied by several researchers earlier (Torrance and Sparrow, 1967). In skin-laser interaction case, the diffusely reflected laser light from the sub-skin layers can convey the skin’s structural information back to the surface and detected by the camera imaging as called laser speckle effect. Whereas the specularly reflected and diffracted (mixed effect) laser light produces very bright image area reflection (Figure 3) which contains no any information. The depth of laser light’s skin penetration depends on its wavelength as such light characteristics have earlier been studied by Bashkatov et al. (2005). In regards to their experiments, the red laser (0.6 nm) light has nearly 2mm penetration capability into the skin and the skin cellular network to be observed by this study is located at the basal layer at approximately 0.1 mm depth of skin (Rice, 2013). All of those operational components take place in a continuous operational loop (Figure 2) for the real-time skin monitoring process.

3 Results and discussion

3.1 Classification test of different subject groups

The experimental stage includes Laser speckle image (LSI) data collection from three different subjects groups, such as: Early vaccinated (starting at 13th February 2021), Late vaccinated (starting at 6th March 2021) and Non-vaccinated individuals for a month period. Camera images are collected from the participants’ forehead regions at the specific time of the day (midnight). Each image sampling size was 30x30 pixels targeting a specific laser speckle-effect region on the images and a single image pixel corresponds to 2.8 microns. Image data set includes 60 cases in total as collected from three subject groups (20 cases for each group) for a month period. The subject groups are labelled as follows: **S**: early vaccinated, **A**: late vaccinated and **E or EM**: non-vaccinated. Laser speckle image samples taken are quantized by textural analysis (Phillips, 1995) as tested earlier (Orun et al., 2014) and then build data sets are processed by Bayesian network for the classification after a training session (by 50/50 ratio of data sets). In the second type of tests, the link discoveries between the data attributes (texture measures of LSI) are found for progressive change detection.

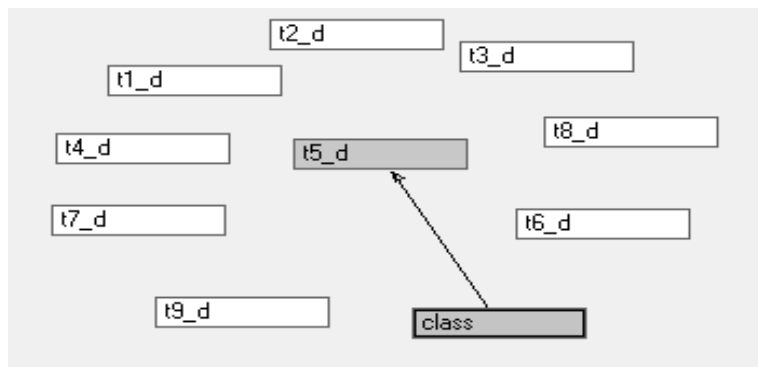


Figure 4. Classification results between the early vaccinated group (S) and the non-vaccinated group (EM) shown in the Bayesian network graph.

The classification has been achieved between the Group (S) and Group (EM) which are early vaccinated and non-vaccinated respectively with 80% classification accuracy results (sensitivity=100%, specificity=60%) (Automatically built network by PowerPredictor™) are presented in Figure 4 with the attribute nodes and connection links. In the network the attributes for Laser image texture measures are symbolized by t_i where classification is achieved over the 5th texture measure. The maximum classification accuracy has been achieved between the Group (A) and Group (EM) which are early vaccinated and non-vaccinated respectively with 90% classification accuracy (Sensitivity = 100%, Specificity = 80%) results as shown in Figure 5.

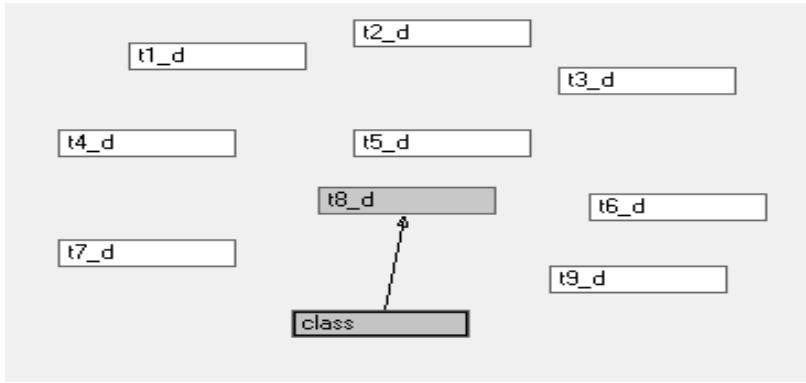


Figure 5. Classification results between the late vaccinated group (A) and the non-vaccinated group (EM) with 90% classification accuracy are obtained via automatically built network by PowerPredictor™. In the network the attributes for Laser image texture measures are symbolized by t_i where classification is achieved over the 8th texture measure (Skewness: 5x5 pixel kernel)

The results show that the parametrically optimized Bayesian classifier called PowerPredictor™ (e.g. by attribute links threshold, discretisation method, single-multi net options, etc.) is capable of discriminating between vaccinated and non-vaccinated individuals (80%-90% classification accuracy) and display the equality between vaccinated individuals (65% classification accuracy).

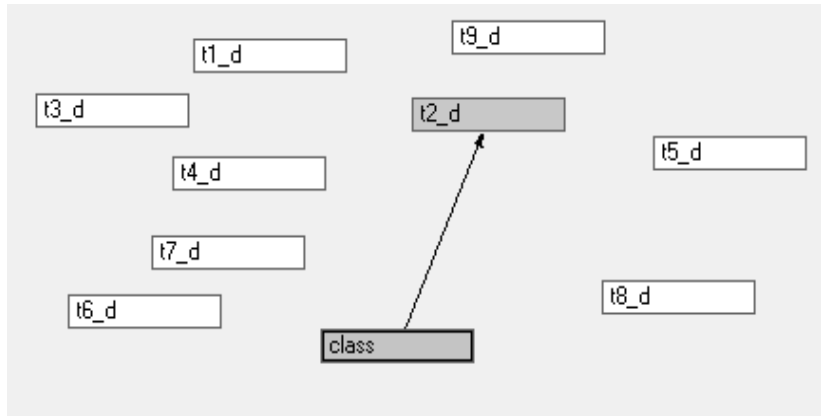


Figure 6. Classification results between the late vaccinated group (A) and the early vaccinated group (S) with 65% classification accuracy are obtained via automatically built network by PowerPredictor™. It is shown that system can not discriminate between those vaccinated groups as expected.

To prove the identical effects of the vaccinations on cellular network structures, similar tests have been carried on with two groups of late vaccinated (group (A) and early vaccinated (group (S) with the results of 65% classification accuracy (Sensitivity = 80%, Specificity = 50%). This meant that the system (with the same network options) could not discriminate between those groups whose automatically constructed Bayesian network is shown in Figure 6.

3.2 Cellular Progressive Changes (CPC) observation test

In the progressive observation test, an artificial progression attribute (e.g. series of numbers between 1-60) is added to each data set to see whether any network link to any other vaccinated individuals' attribute will be established automatically by a specific Bayesian tool PowerConstructor™. To prove that there is a progress of changes on a cellular network or cellular properties. This would be any change in cellular network structure in shape, an increase of antibodies in the blood (micro-veins) or any other cellular/subcellular content. In the results, the system establishes a link between the progression attribute and vaccinated groups (S, A) but not displays any link between the progression attribute and the non-vaccinated group (E) as shown in Figure 7.

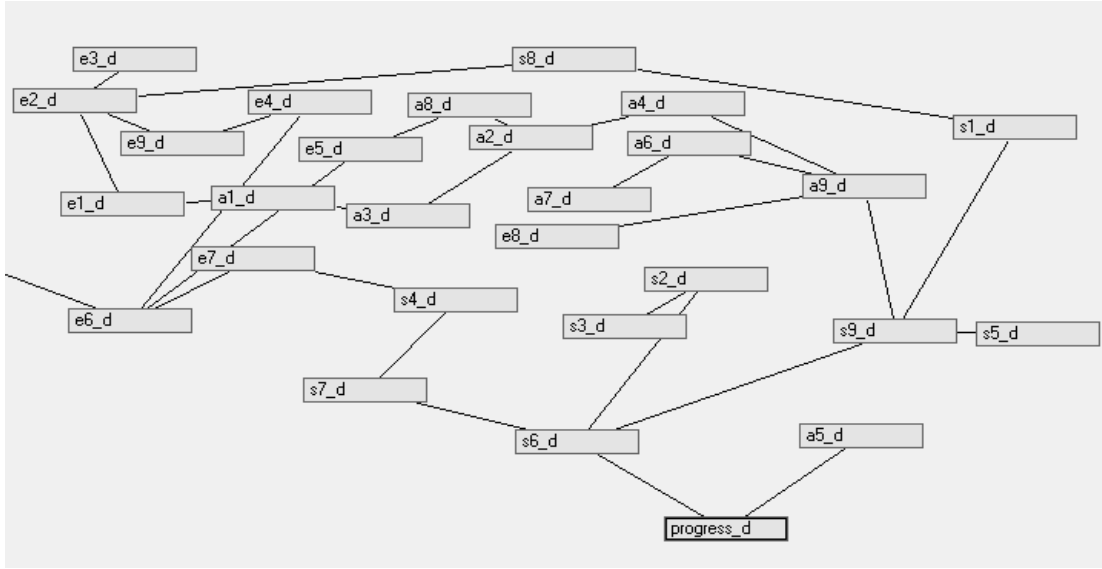


Figure 7. The Bayesian inference system (PowerConstructor™) analyse the whole data set and connects the links between the “cellular progressive change” attribute and vaccinated groups (S: early-vaccinated and A:late-vaccinated) but no any link to non-vaccinated group E is established.

The Partial data set shown in Table 1 includes texture $t_1 - t_9$ calculations referring to pixel based statistics formulated in Figure 3 with two arithmetic operator (pixel kernel) groups as are 3x3 and 5x5 pixels. Table 1 also includes an artificially built “progressive change” attribute in the last column to investigate if there is any link between any of the attributes and progression measures.

Table I. Partial data set including the textural attributes ($t_1 - t_9$) and artificially built “progressive change” attribute (progress) shown in the last column with a regular increment. The Class column includes all classes but here only single class (S: early-vaccinated) is shown due to limited “partially” display of whole data set normally including Groups A and E.

| t1 | t2 | t3 | t4 | t5 | t6 | t7 | t8 | t9 | class | progress |
|-----|-----|-------|------|-----|----|------|------|-------|-------|----------|
| 565 | 684 | 26.15 | 3.51 | 97 | 96 | 9.8 | 0.16 | 17.59 | S | 1 |
| 568 | 612 | 24.74 | 3.89 | 66 | 25 | 5 | 0.52 | 16.39 | S | 2 |
| 571 | 643 | 25.36 | 3.71 | 81 | 58 | 7.62 | 0.63 | 17.01 | S | 3 |
| 571 | 629 | 25.08 | 3.75 | 82 | 49 | 7 | 0.48 | 16.83 | S | 4 |
| 571 | 643 | 25.36 | 3.68 | 99 | 63 | 7.94 | 0.52 | 17.11 | S | 5 |
| 571 | 640 | 25.3 | 3.75 | 79 | 49 | 7 | 0.38 | 16.88 | S | 6 |
| 563 | 598 | 24.45 | 3.84 | 80 | 31 | 5.57 | 0.93 | 16.36 | S | 7 |
| 568 | 646 | 25.42 | 3.72 | 85 | 54 | 7.35 | 0.24 | 16.93 | S | 8 |
| 571 | 659 | 25.67 | 3.57 | 109 | 88 | 9.38 | 0.68 | 17.52 | S | 9 |
| 571 | 649 | 25.48 | 3.69 | 89 | 60 | 7.75 | 0.83 | 16.94 | S | 10 |
| 571 | 613 | 24.76 | 3.86 | 66 | 32 | 5.66 | 0.07 | 16.53 | S | 11 |
| 571 | 637 | 25.24 | 3.73 | 83 | 54 | 7.35 | 0.36 | 16.95 | S | 12 |
| 568 | 618 | 24.86 | 3.79 | 88 | 44 | 6.63 | 0.98 | 16.75 | S | 13 |
| 571 | 634 | 25.18 | 3.75 | 80 | 48 | 6.93 | 0.48 | 16.83 | S | 14 |

Conclusion

The proposed potential use of Intelligent laser Speckle Classification (ILSC) in association with the Bayesian Inference and classification techniques is the unique one among the other conventional methods like immunoglobulin tests, as *ILSC* optimally unifies different disciplinary fields like light physics, texture analysis and AI method to outperform the other conventional techniques in terms of speed, non-invasiveness and real-time functionality. The most common methods used to observe Covid-19 vaccines effects rely on the immunoglobulin test which checks the amount of certain antibodies called immunoglobins generated progressively in the body. The antibodies are proteins that immune cells produce to fight against viruses. The proposed ILSC technique may also be utilized to observe the prognosis period of Covid-19 disease with the possible healing effect of particular substances (e.g. Dexamethasone (NHS England, 2021), Remdesivir (Dyer, 2020), Regn-Cov2 (Weinreich et al., 2021), etc.) at high frequency of tests. It can also be potentially used to select the most effective vaccine type for the individual (in the concept of personalised medicine (Vogenberg, 2010) by a frequent observation of the vaccine

effect on the body tissue cells. The proposed system is getting more inevitable by its unique characteristics like its instant use even at the real-time speed as well as its flexible re-design capacity of instrumentation such as specifically selection of its laser wavelength suitable with the size of observation features (e.g. sub-cellular components), power of laser source to adjust its light penetration into the skin layers, camera resolution and another AI method used (e.g. Convolutional neural networks, etc.). The system reliability would be further increased by next advanced version of the proposed technique called “Multi-Classifier System” (MCS) by the addition of more laser sources with different wavelengths (e.g. red, IR, etc.). Further improvement of the system capability (e.g. blood clot development risk assessment after vaccination) would depend on such data collection procedure from the specific patient group who suffer from blood clot development issue, as technical configuration of proposed system would be capable enough to overcome such task with some minor system modifications like laser wavelength selection sensitive to subtle changes of blood content, circulation velocity, etc. The low-cost and highly portable characteristics of the system is promising for its broad usage in the health community, transport environments, leisure centres, schools, etc.

Declarations

Competing Interests

There is no any financial or personal competing interest available.

Authors' contributions

The corresponding author Ahmet Orun has achieved the data collection, developed the experimental tools and manuscript. Co-author Fatih Kurugollu has reviewed the paper, data analysis and made some supplementary works.

Funding

No any funding has received for the research

References

AstraZeneca, <https://www.astrazeneca.com>. Oxford, United Kingdom. 2021.

Bashkatov, A.N., E.A. Genina, V.I. Kochubey and V.V. Tuchin. Optical properties of human skin, subcutaneous and mucous tissues in the wavelength range from 400 to 2000nm. *J. Phys.D:Appl. Phys.*38(2005),pp.2543-2555.

Bogdanov, G., I. Bogdanov, J. Kazandjieva, N.Tsankov. Cutaneous adverse effects of the available Covid- 19 vaccines. *Clinics in Dermatology*, Article in press, 2021.

Butkus BD. Blood-flow imaging adapted for endoscopy. *Biophotonics Int* 2003; 10: 17–20.

Dainty C. Laser speckle and related phenomena. Berlin, SpringerVerlag: 1984.,ISBN 0-387-13169-8

Drugan MM, Wiering MA. Feature selection for Bayesian networks classifiers using the MDL-FS score. *Int J Approximate Reasoning* 2010; 51: 695–717.

Dyer, O. Covid-19: Remdesivir has little or no impact on survival, WHO trial shows. *BMJ* 2020, 371:m4057.

Ginouves P. The next generation of analytical instruments. *Biophotonics Int* 2003; 10: 48–54.

Ho, T., Hull JJ, Srihari S. Decision combination in multiple classifier systems. *IEEE Trans Pattern Anal Mach Intell.* 1994;16(1):66–75.

Jensen F. An introduction to Bayesian networks. NewYork: Springer; 1998.

Ledford, H., D. Cyranoski, R. Van Noorden. The UK has approved a COVID vaccine - here's what scientists now want to know. *Nature*, 588 (2020), pp. 205-206

Lospinoso, K., C.S. Nichols, S.J. Malachowski, M.C. Mochel and F. Nutan. A case of severe cutaneous adverse reaction following administration of the Janssen ad.26.cov2.s Covid-19 vaccine. *JAAD Case*

Reports 2021; 13: 134-7.

Magro, C., G.Nuovo, J. Mulvey, J. Laurence, J. Harp and N. Crowson. The skin as a critical window in unveiling the pathophysiologic principles of Covid-19, *Clinics in Dermatology*, Article in Press, 2021 <https://doi.org/10.1016/j.clindermatol.2021.07.001>

McMahon, D.E., E. Amerson, M. Rosenbach, *et al.* Cutaneous reactions reported after Moderna and Pfizer COVID-19 vaccination: a registry-based study of 414 cases. *J Am Acad Dermatol*, 85 (1) (2021), pp. 46-55

Millet C, Roustit M, Blaise S, Cracowski JL. Comparison between laser speckle contrast imaging and laser Doppler imaging to assess skin blood flow in humans. *Microvasc Res* 2011; 82: 147–151.

Mohamed, S., K. Saad, G. Elgohary, A. Abdelhaffes and N. Abdelaziz. IS Covid-19 a systemic disease ?, *Coronaviruses*, Vol.2, Issue 5, 2021.

NHS England, Covid treatment developed in the NHS saves a million lives. 23 March 2021. <https://www.england.nhs.uk/2021/03/covid-treatment-developed-in-the-nhs-saves-a-million-lives>

Orun, A.B and Alkis, A. “Material identification by surface reflection analysis in Combination with Bundle Adjustment Technique”, *Pattern Recognition Letters*, Elsevier Science, Vol. 24, No. 9-10, June 2003.

Orun AB, Seker H. Development of a computer game-based framework for cognitive behaviour identification by using Bayesian inference methods. *Comp Hum Behav* 2012; 28: 1332–1341.

Orun, A.B, E. Goodyer, H.Seker, G. Smith, V.Uslan And D. Chauhan, (2014) “Optimized parametric skin modelling for diagnosis of skin abnormalities by combining light back-scatter and laser speckle imaging”, *Skin Research and Technology*, 2014; 1-13.

Orun, A.B., Non invasive imaging method promising for skin assessment, *Photonics Spectra*, Vol.16 (4), April 2014. (Press News article)

Orun, A.B, Seker, H., V.Uslan, E.Goodyer and G.Smith. (2016) Texture based characterization of sub-skin features by specified laser speckle effects at $\lambda=650\text{nm}$ region for more accurate parametric “skin age” modelling. *International Journal of Cosmetic Science*. 2016 (1-7).

Orun, A.B and G.Smith (2017) Micro-structural analysis of tablet surface layers by intelligent laser speckle classification (ILSC) technique: An application in the study of both surface defects and subsurface granule structures. *Journal of Pharmaceutical Innovation*.Vol.12, No.4

Phillips D. Image processing in C, part 15: basic texture operations. *C/C++ Users J* 1995; 13: 55–68.

Rice, A.N. Rice, A.N. Laser microscopy tests for skin damage. *Bio Photonics*. <http://www.photonics.com/Article.aspx?AID=53291>, March (2013).

Sun, Q., R. Fathy, D. E. McMahon and E.E. Freeman, Covid-19 vaccines and the skin: the landscape of cutaneous vaccine reactions worldwide, *Dermatologis Clinics*, Article In Press, 2021, <https://doi.org/10.1016/j.det.2021.05.016>

Torrance, K. and E. Sparrow. Theory of off-specular reflection from roughened surfaces. *J. Opt. Soc. Am. A*. 1967; 57:1105-14.

Tregoning, J.S., E.S. Brown, H.M. Cheeseman, *et al.* Vaccines for COVID-19, *Clin Exp Immunol*, 202 (2020), pp. 162-192

Vogenberg, F.R., C.I. Brash and M. Pursel. Personalised Medicine. *Pharmacy & Therapeutics*, 2010, 35(10). pp. 560-562.

Voysey, M., S.A.C. Clemens, S.A. Madhi, *et al.* Safety and efficacy of the ChAdOx1 nCoV-19 vaccine (AZD1222) against SARS-CoV-2: an interim analysis of four randomised controlled trials in Brazil, South Africa, and the UK. *Lancet*, 397 (2021), pp. 99-111

Weinreich, D.M., S.Sivapalasingam, T. Norton, S. Ali, H. Gao, R. Bhore, B. Musser, Y. Soo, D. Rofail, J. Im, C. Perry, C. Pan, et al. REGN-COV2, a Neutralizing Antibody Cocktail, in Outpatients with Covid-19. *The New England Journal of Medicine*, 2021; 384:238-251.

World Health Organisation. Coronavirus Disease (Covid-19): Vaccines. WHO Archive: December 2020.

Wozniak M, Grana M, Corchado E. A survey of multiple classifier systems as hybrid systems. *Information Fusion*. 2014;16:3–17. 23.

Zhao, Q., X Fang, Z Pang, B Zhang, H Liu, F. Zhang. COVID-19 and cutaneous manifestations: a systematic review. *J Eur Acad Dermatol Venereol*, 34 (2020), pp. 2505-2510.